1 Imaginary Wilson coefficients and R_K observables

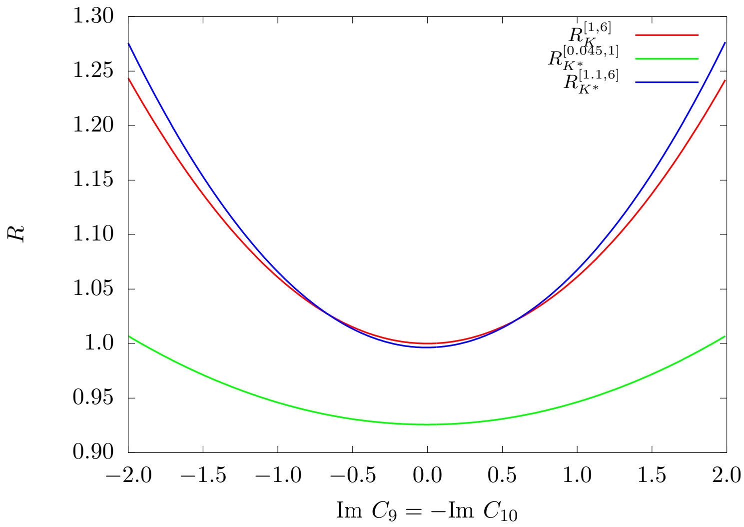

Figure 1: Values of R_K and R_{K^*} whith imaginary Wilson coefficients.

Figure **??** shows the values of the ratios R_K and R_{K^*} in their respective q^2 ranges, when both Wilson coefficients C_9 and C_{10} are imaginary, and also we assume $C_9 = -C_{10}$. In all cases the minimum value for the ratio is attained at the SM point $C_9 = -C_{10} = 0$. The addition of non-zero imaginary Wilson coefficients results in larger values of R_K and R_{K^*}, at odds with the experimental values $R_{K^{(*)}}^{\mathrm{exp}} < R_{K^{(*)}}^{\mathrm{SM}}$.

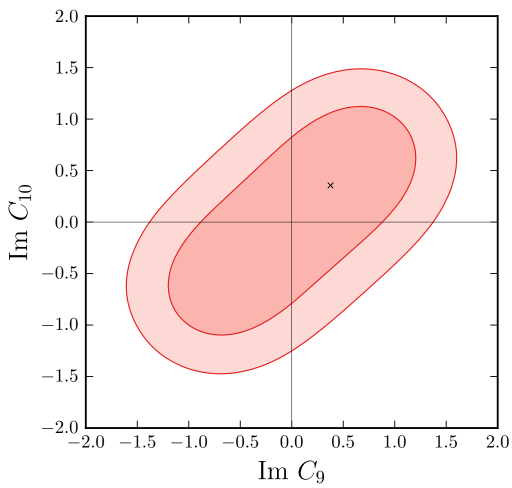

Figure 2: Allowed regions for imaginary Wilson coefficients.

In Figure **??** we plot the allowed regions for imaginary values of C_9 and C_{10} when fitting to measurements of a series of $b \to s\mu^+\mu^-$ observables. In the fit we have included the ratios R_K and R_{K^*}, the angular observables P_4' and P_5' and the branching ratios $\mathrm{BR}(B_s \to \mu^+\mu^-)$ and $\mathrm{BR}(B^0 \to \mu^+\mu^-)$. The fit was carried by the software `flavio`, wich computes the χ^2 function with each (C_9, C_{10}) pair. The global minimum of the χ^2 was found at $C_9 = 0.31\,i$, $C_{10} = 0.29\,i$. The pull of the SM, defined as the probability that the SM scenario can describe the best fit assuming that $\Delta\chi^2 = \chi^2_{\mathrm{SM}} - \chi^2_{\mathrm{min}}$ follows a χ^2 distribution with 5 degrees of freedom, is of just $2.1 \times 10^{-5}\sigma$. That is, the SM result and the best fit are indistinguishable from an statistical point of view. The shaded regions in the plot are 1σ (darker pink) and 2σ (lighter pink) away from the best fit.

2 Z' fit

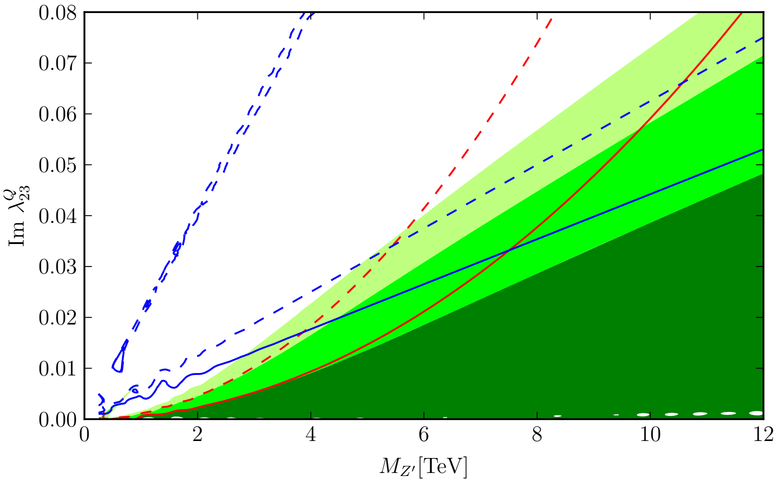

Figure 3: Bounds on Z' parameter space imposed by $b \to s\mu^+\mu^-$ decays and B_s mixing.

Figure **??** shows the bounds on the Z' mass $M_{Z'}$ and the imaginary coupling coupling λ_{23}^Q (setting $\lambda_{22}^L = 1$) imposed by $b \to s\mu^+\mu^-$ decays and B_s mixing. Blue lines correspond to the fit to B_s-mixing observables ΔM_s and $A_{\rm CP}^{\rm mix}$ (solid line: $\Delta\chi^2 = 1$, dashed lines $\Delta\chi^2 = 4$), red lines to $b \to s\mu^+\mu^-$ as in Figure **??** (solid line: $\Delta\chi^2 = 1$, dashed lines $\Delta\chi^2 = 4$), and green regions to the combined fit (dark green: $\Delta\chi^2 = 1$, medium green $\Delta\chi^2 = 4$, light green: $\Delta\chi^2 = 9$). For the B_s-mixing fit, the SM offers the best fit, while the best fits for the $b \to s\mu^+\mu^-$ and global fits is ($M_{Z'} = 11.0$ TeV, $\lambda_{23}^Q = 0.001i$), although the improvement with respect to the SM is negligible. In the low mass region ($M_{Z'} \lesssim 7$ TeV) the global fit is dominated by $b \to s\mu^+\mu^-$ observables, and B_s-mixing becomes more important at larger masses. The allowed regions correspond to 'small' Wilson coefficients (Im$C_{10} < 0.7$, $C_{bs}^{LL} > -3 \times 10^{-4}$), except for a narrow region in the B_s fit with $C_{bs}^{LL} \sim -2.7 \times 10^{-3}$.

3 Leptoquark fit

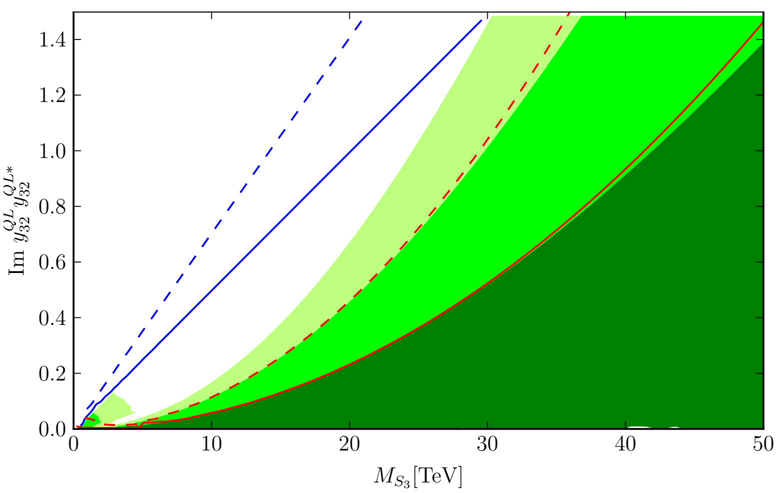

Figure 4: Bounds on S_3 leptoquark parameter space imposed by $b \to s\mu^+\mu^-$ decays and B_s mixing.

Figure **??** shows the bounds on the S_3 leptoquark mass M_{S_3} and the imaginary coupling coupling $y_{23}^{QL} y_{23}^{QL*}$ imposed by $b \to s\mu^+\mu^-$ decays and B_s mixing. The observables used in the respective fits are the same as in Figure **??**. The SM scenario was prefered in all the fits. In contrast to Z' models, $b \to s\mu^+\mu^-$ observables remain the main contributors to the bounds at masses as large as $M_{S_3} \sim 50$ TeV.